

Strengthening of RC Members Using Near-Surface Mounted FRP Composites: Design Overview

Renato Parretti¹ and Antonio Nanni²

ABSTRACT

Strengthening of reinforced and prestress concrete (RC and PC) members using externally bonded FRP laminates is today a well-accepted technology that is becoming popular among designers and contractors. Near-surface mounted FRP reinforcement represents an alternative way to improve flexural and shear performance of concrete structures. In some instance, it is the only suitable technology that can be efficiently applied, for example, when upgrading beam-column joints or for the flexural strengthening of compression members.

In this paper, bond related issues, flexural and shear design recommendations, and design examples are discussed and proposed. The paper is an attempt to provide designers with the first comprehensive protocol for the rational implementation of the technology.

KEY WORDS:

Bond, Detailing, Flexural Design, FRP, Near-Surface Mounted Reinforcement, Reinforced Concrete, Shear Design, Strengthening

INTRODUCTION

The use of Near-Surface Mounted (NSM) FRP reinforcement is an attractive method for increasing the flexural and shear strength of deficient RC and PC members (Alkhrdaji et al., 1999, De Lorenzis et al., 2000) as well as strengthening unreinforced masonry walls (Tumialan et al. 2001). Advantages with respect to externally bonded FRP laminates include the possibility of anchoring the reinforcement into adjacent members, and the opportunity of upgrading elements in their negative moment region with the reinforcement not exposed to potential mechanical damage typical of floor or deck systems (Nanni et al. 1999). The NSM FRP technique does not require extensive surface preparation work, and after groove cutting, requires minimal installation time compared to externally bonded FRP laminates.

The NSM reinforcement technology becomes particularly interesting in seismic retrofit of RC column-beam joints providing either additional strength or ductility when moving the failure zone from the column to the beam (Prota et al., 2001).

Figure 1 shows a recent application of NSM technology for silo strengthening (Emmons et al., 2001) where FRP bars have been used to enhance both flexural and confinement capacity. Figure 2 illustrates the application of this technology for upgrading a solid RC bridge deck (Alkhrdaji et al., 2000), and Figure 3 represents a

¹ Structural Engineer, Co-Force America Inc., USA.

² V&M Jones Professor of Civil Engineering, University of Missouri-Rolla, USA.

similar case where NSM bars were used to increase the bridge deck negative moment capacity (Warren, 1998). Figure 4 shows shear strengthening of RC joists enhanced with Carbon FRP bars used as Near-Surface Mounted reinforcement (Hogue et al., 1999).

HISTORY OF THE TECHNOLOGY

The use of NSM reinforcement was developed in Europe for strengthening of RC structures in the early 1950s. In 1948, an RC bridge deck in Sweden needed to be upgraded in its negative moment region due to an excessive settlement of the steel cage during construction. This was accomplished by inserting steel reinforcement bars in grooves made in the concrete surface and filling it with cement mortar (Asplund, 1949).

More recently, NSM reinforcement has been used to upgrade masonry structures to increase their tensile strength and ductility (Atkinsosn and Shuller, 1992). This technology is an effective and economical means of repairing and strengthening low-rise masonry buildings and arch bridges (Garrity, 1995). Stainless steel has replaced the original black steel adopted at the onset of the development, while the cementitious grout used for embedding the reinforcement has been partially replaced by epoxy-based grouts.

Today, FRP bars have become attractive for their non-corrosive properties and the ability of tailoring the bar stiffness to the needs of the application. Epoxy-based pastes or later-modified cement grouts can be used for their rapid setting and bond strength.

DESIGN PHILOSOPHY

The strength design approach with its strength reduction factors as used in ACI 318 (1999) is recommended for RC and PC members using NSM FRP reinforcement. Additional strength reduction factors applied to the contribution of the NSM reinforcement are suggested to reflect the novelty of FRP systems compared with traditional methods.

The equations presented in this paper are based on principles of force equilibrium, strain compatibility, constitutive laws of the materials, and make reference to the “Guide for the Design and Construction of Externally Bonded FRP Systems for Strengthening Concrete Structures” reported by ACI Committee 440 (2002), and the “Guide for the Design and Construction of Concrete Reinforced with FRP Bars” also reported by ACI Committee 440 (2001).

Careful consideration should be given to determine a strengthening threshold. The threshold is imposed to guard against collapse of the structure should bond or other failure of the FRP system occur due to fire, vandalism, or other causes. The existing strength of the structure (ϕR_n) should be sufficient to resist a level of load described by Eq. (1):

$$(\phi R_n)_{existing} = (1.2D + 0.85L)_{new} \quad (1)$$

Material properties of the FRP reinforcement reported by manufacturers, such as the ultimate tensile strength, typically do not consider long-term exposure to environmental conditions, and should be considered as initial properties. FRP properties to be used in all design equations are given as follows (ACI 440, 2001, and 2002):

$$\begin{aligned} f_{fu} &= C_E f_{fu}^* \\ \varepsilon_{fu} &= C_E \varepsilon_{fu}^* \end{aligned} \quad (2)$$

where f_{fu} and ε_{fu} are the FRP design tensile strength and ultimate strain considering the environmental reduction factor (C_E) as given in Table 1, and f_{fu}^* and ε_{fu}^* represent the FRP guaranteed tensile strength and ultimate strain as reported by the manufacturer. FRP design modulus of elasticity is the guaranteed value reported by the manufacturer.

FLEXURAL DESIGN

Guidance for the calculation of the flexural strengthening effect resulting from longitudinal FRP reinforcement mounted onto the tension face of an RC member is illustrated in Figure 5 for the case of a rectangular section.

Assumptions used in the design are: *a)* a plane section before loading remains plane after loading; *b)* the maximum usable compressive strain in the concrete is 0.003 , and its tensile strength is neglected; *c)* the FRP reinforcement has a linear-elastic behavior up to failure; and *d)* perfect bond exists between FRP reinforcement and surrounding concrete.

The strength reduction approach follows the philosophy of ACI 318 (1999) Appendix B, where a member with low ductility should be compensated with a higher strength reserve. The higher strength reserve is achieved by applying a factor of 0.70 to brittle members, as opposed to 0.90 for ductile members. The strength-reduction factor (ϕ) given by Eq. (3) should be used (ACI 440, 2002):

$$\phi = \begin{cases} 0.90 & \text{for } \varepsilon_s \geq 0.005 \\ 0.70 + \frac{0.20(\varepsilon_s - \varepsilon_y)}{0.005 - \varepsilon_y} & \text{for } \varepsilon_y < \varepsilon_s < 0.005 \\ 0.70 & \text{for } \varepsilon_s \leq \varepsilon_y \end{cases} \quad (3)$$

where ε_s and ε_y is the strain in the reinforcing steel at ultimate and yielding, respectively.

The calculation procedure used to arrive at the ultimate strength should consider the governing mode of failure. The trial and error procedure presented in this paper involves selecting a given neutral axis depth (c) and a failure mode (i.e. selecting $\varepsilon_c = \varepsilon_{cu}$ or $\varepsilon_f = \varepsilon_{fe}$); calculating the strain level in each material using strain compatibility; calculating the associated stress level in each material from its stress-strain relationship; and checking internal force equilibrium. If the internal force resultants do not equilibrate, the depth to the neutral axis is revised and the procedure repeated.

When failure is controlled by concrete crushing, the Whitney stress block approach (ACI 318, 1999) can be used without modifications. If FRP rupture or concrete cover delamination control failure, the Whitney stress block gives reasonably accurate results provided that α_l take the expression of Eq. (4) rather than the fixed value of 0.85 (while β_l remains the same as from Section 10.2.7.3 of ACI 318, 1999):

$$\alpha_1 = \frac{3\varepsilon_c' \varepsilon_c - \varepsilon_c^2}{3\varepsilon_c'^2 \gamma_1} \quad (4)$$

where:

$$\varepsilon_c' = 1.71 \frac{f_c'}{E_c} \quad (5)$$

$$\gamma_1 = \frac{4\varepsilon_c' - \varepsilon_c}{6\varepsilon_c' - 2\varepsilon_c}$$

The ultimate effective strain (ε_{fe}) that should be used for FRP reinforcement is given below:

$$\varepsilon_{fe} = \kappa_m \varepsilon_{fu} \quad (6)$$

where κ_m is a bond dependent coefficient meant to limit the strain in the FRP reinforcement to prevent debonding or delamination. Limited experimental evidences (De Lorenzis and Nanni, 2002) indicate that κ_m is highly affected by surface properties of the FRP bar (deformed or sandblasted), by groove size, by properties of the epoxy paste, and concrete tensile strength. Splitting of the epoxy cover, cracking of the concrete surrounding the bar, and pull-out of the FRP bar were the main failure modes experimented during the laboratory tests reported in the literature. Experimental values of κ_m were found to vary between 0.60 and 0.84. Further research should result in a more accurate method for predicting the appropriate bond dependant factor. A value of $\kappa_m=0.70$ has been selected in the design example (see Appendix I). This value is consistent with both experimental data (De Lorenzis and Nanni, 2002) and the approach followed by ACI 440 (2002) when defining an equivalent strain reduction factor for externally bonded FRP laminates.

Nominal tension strain attained in the concrete surrounding FRP bars can be expressed as:

$$\varepsilon_{c,f} = \frac{d_f - c}{c} \varepsilon_{cu} \leq \varepsilon_{fe} + \varepsilon_{bi} \quad (7)$$

where d_f represents the depth to the FRP reinforcement as illustrated in Figure 5,

The initial strain ε_{bi} in Eq. (7) can be evaluated using an elastic analysis of the existing member, considering all loads present at the time of FRP installation. The first term in Eq. (7), $\frac{d_f - c}{c} \varepsilon_{cu}$, should be used when concrete crushing failure governs. The second term, $\varepsilon_{fe} + \varepsilon_{bi}$, should be used when FRP is the controlling failure mode.

Assuming no compression steel reinforcement, the moment capacity of the strengthened member can be expressed as follows:

$$M_n = A_s f_s \left(d - \frac{\beta_1 c}{2} \right) + \psi_f A_f f_{fe} \left(d_f - \frac{\beta_1 c}{2} \right) \quad (8)$$

where f_s and f_{fe} are taken from Eq. (9), and ψ_f is an additional reduction factor of 0.85 recommended to take into account for the novelty of FRP (ACI 440, 2002):

$$\begin{aligned} f_s &= E_s \varepsilon_s < f_y \\ f_{fe} &= E_f \varepsilon_{c,f} \leq E_f \varepsilon_{fe} \end{aligned} \quad (9)$$

SHEAR DESIGN

The approach used to calculate the nominal shear capacity of a member strengthened using NSM bars is similar to that used in ACI 440 (2002) for the case of externally bonded FRP laminates. Eq. (10) is applicable for NSM systems and the same strength reduction factor $\phi=0.85$ suggested by ACI 318 is used. An additional reduction factor $\psi_f=0.85$ is applied to the contribution of NSM FRP reinforcement to the shear strength of the member, as previously suggested for flexural design.

$$\phi V_n = \phi(V_c + V_s + \psi_f V_f) \quad (10)$$

Several parameters influence the NSM FRP bars contribution to the shear capacity (V_f), such as quality of bond, FRP rebar type, groove dimensions, and quality of substrate material. When computing V_f , two strain limits need to be taken into account (De Lorenzis and Nanni, 2001a) namely: strain from bond-controlled failure, and maximum strain threshold of 0.004. The latter is suggested to maintain the shear integrity of the concrete (Khalifa et al., 1998), and to avoid large shear cracks that could compromise the aggregate interlock mechanism.

The following assumptions are made: *a*) the slope of the shear crack is assumed to be at 45 degrees; and *b*) bond stresses are constant along the effective length of the FRP bar at ultimate.

The shear strength provided by the NSM reinforcement can be determined by calculating the force resulting from the tensile stress in the FRP bars across the assumed crack, and it is expressed by Eq. (11) for circular and rectangular bars, respectively.

$$\begin{aligned} V_f &= 2\pi d_b \tau_b L_{tot} \\ V_f &= 4(a+b)\tau_b L_{tot} \end{aligned} \quad (11)$$

where d_b is the nominal FRP bar diameter, a and b represent the cross-sectional dimension for rectangular FRP bar, and τ_b represents the average bond stress of the bars crossed by a shear crack. Experimental data available on 10-mm (#3) carbon FRP deformed bars demonstrate that when using an epoxy based resin in a groove size at least 1.5 times the bar diameter, a conservative value of $\tau_b=6.9 \text{ MPa}$ (1.0 ksi) can be used (De Lorenzis and Nanni, 2001b).

L_{tot} can be expressed as $L_{tot} = \sum_i L_i$ where L_i (Figure 12) represents the length of each single NSM bar crossed by a 45-degree shear crack expressed as follows:

$$L_i = \begin{cases} \frac{s}{\cos \alpha + \sin \alpha} i \leq l_{0.004} & i = 1 \dots \frac{n}{2} \\ \ell_{net} - \frac{s}{\cos \alpha + \sin \alpha} i \leq l_{0.004} & i = \frac{n}{2} + 1 \dots n \end{cases} \quad (12)$$

where α is the slope of the FRP bar with respect to the longitudinal axis of the member (common values are 90° for vertical NSM bars, and 45° or 60° for inclined bars), s is the FRP bar spacing, and ℓ_{net} , defined as follows:

$$\ell_{net} = \ell_b - \frac{2c}{\sin \alpha} \quad (13)$$

represents the net length of a FRP bar as shown in Figure 12 to account for cracking of the concrete cover and installation tolerances. In Eq. (13), ℓ_b is the actual length of a FRP bar, and c is the clear concrete cover of the internal longitudinal reinforcement.

The second limitation in Eq. (12), $l_{0.004}$, takes into account the shear integrity of the concrete by limiting at 0.004 the maximum strain in the FRP reinforcement. From the force equilibrium condition, ($A_b(0.004E_f) = \pi d_b l_{0.004} \tau_b$), $l_{0.004}$ can be determined as follows for circular and rectangular bars, respectively:

$$l_{0.004} = 0.001 \frac{d_b E_f}{\tau_b} \quad (14)$$

$$l_{0.004} = 0.002 \frac{a \cdot b E_f}{a + b \tau_b}$$

where E_f represents Young's modulus of FRP bars.

The first limitation in Eq. (12) takes into account bond as the controlling failure mechanism, and represents the minimum effective length of an FRP bar crossed by a shear crack. It is expressed by $s \cdot i / (\cos \alpha + \sin \alpha)$ or $\ell_{net} - s \cdot i / (\cos \alpha + \sin \alpha)$ depending on the value assumed by the term

$$n = \frac{\ell_{eff}(1 + \cot \alpha)}{s} \quad (15)$$

where n is taken as the smallest integer (e.g., $n = 32/3 = 10.7 \Rightarrow n = 10$), and ℓ_{eff} represents the vertical length of ℓ_{net} written as follows:

$$\ell_{eff} = \ell_b \sin \alpha - 2c \quad (16)$$

Spacing of FRP shear reinforcement should not exceed $l_{net}/2$, or 24 in.

To prevent crushing of concrete, the total reinforcement contribution taken as the sum of both steel and FRP reinforcement, should be limited based on the criteria given for steel alone in ACI 318, as suggested in Eq. (17) for US and SI customary, respectively:

$$V_s + V_f \leq \begin{cases} 8\sqrt{f'_c}bd \\ 0.66\sqrt{f'_c}bd \end{cases} \quad (17)$$

DETAILING

The minimum dimension of the grooves should be taken at least 1.5 times the diameter of the FRP bar. However, when a rectangular bar with large aspect ratio is used, the limit may lose significance due to constructability. In such a case, a minimum groove size of $3.0a \times 1.5b$ as depicted in Figure 8 could be suggested, where a is the smallest bar dimension. In other instances, the minimum groove dimension could be the result of installation requirements rather than engineering. For example a 5 mm (0.2 in) groove may be the smallest possible because of the saw blade size.

Bond properties between FRP reinforcement and concrete are similar to that of steel reinforcement, and depend on FRP type, elastic modulus, surface deformation, and shape of the FRP bar (Al-Zahrani et al., 1996, Uppuluri et al., 1996, Gao et al., 1998). For the case of RC beams strengthened using NSM CFRP rectangular bars, Hassan and Rizkalla (2002) found that the development length is highly dependent on strip dimensions, groove size, concrete and adhesive properties, internal steel reinforcement ratio, reinforcement configuration, and type of loading. They suggested that the development length increases by increasing the internal steel reinforcement ratio, and decreases with the increase of either the concrete compressive strength and/or the groove size.

Figure 9 shows the equilibrium condition of an FRP bar with an embedded length equal to its development length, l_d . The force in the bar is resisted by the shear stresses τ_b acting on the surface of the bar. Assuming a triangular stress distribution (Ibell and Valerio, 2002), the average bond stress can be expressed as $\tau_b = 0.5 \tau_{max}$.

Via equilibrium, the following equations can be derived for circular and rectangular bars, respectively:

$$l_d = \frac{d_b}{4(0.5\tau_{max})} f_{fe} \quad (18)$$

$$l_d = \frac{a \cdot b}{2(a+b)(0.5\tau_{max})} f_{fe}$$

Hassan and Rizkalla (2002) suggest an expression for τ_{max} when concrete crushing is the controlling failure mode. When the controlling failure mode is not known, a conservative value of $\tau_{max}=3.5 \text{ MPa}$ (0.50 ksi) is suggested.

CONCLUSIONS

Near-surface mounted reinforcement is an old technology used over more than half a century to enhance flexural and shear capacity of existing RC and masonry structures. Today, thanks to the availability of FRP composites, it is becoming increasingly more attractive and sometimes even more promising than the use of externally bonded FRP laminates.

In this paper, an overview of flexural and shear design of RC members strengthened with NSM FRP bars was presented. The proposed procedure reflects the framework used in the two guides published by ACI (ACI 440, 2002, and ACI 440.1R-01, 2001) with adjustment coming from experimental evidences.

Unresolved issues requiring additional experimental work include properties and quality of bond between FRP bars, paste and concrete, as well as a better understanding of the importance of groove size, especially when using rectangular bars. Limited experience is available on shear strengthening with NSM bars, and more data are needed to better validate the analysis here presented.

REFERENCES

ACI Committee 318, 1999; "Building Code Requirements for Structural Concrete (ACI 318-99) and Commentary (ACI 318R-99)", *American Concrete Institute*, Farmington Hills, Michigan, 391 pp.

ACI Committee 440, 2002; "Guide for the Design and Construction of Externally Bonded FRP Systems for Strengthening Concrete Structures", *American Concrete Institute*, Farmington Hills, Michigan, *in press*.

ACI Committee 440, 2001; "Guide for the Design and Construction of Concrete Reinforced with FRP Bars (ACI 440.1R-01)", *American Concrete Institute*, Farmington Hills, Michigan, 41 pp.

Alkhrdaji, T., Nanni, A., Chen, G., and Barker, M. (1999), "Upgrading the Transportation Infrastructure: Solid RC Decks Strengthened with FRP," *Concrete International*, American Concrete Institute, Vol. 21, No. 10, pp. 37-41.

Alkhrdaji, T., Nanni, A., and Mayo, R., 2000; "Upgrading Missouri Transportation Infrastructures: Solid RC Decks Strengthened with FRP", *Transportation Research Record*, No. 1740, pp. 157-169. (also available in: *Proc., 79th Annual Transportation Research Board*, Jan. 9-13, 2000, Washington, DC, CD-ROM version, paper 00-1177, 24 pp.)

Al-Zahrani, M.M., Nanni, A., Al-Dulaijan, S.U., and Bakis, C.E., 1996; "Bond of FRP to Concrete for Bars with Axisymmetric Deformations", *Proceedings of the Second International Conference on Advanced Composite Materials in Bridges and Structures (ACMBS-II)*, Montreal, Canada, pp. 853-860.

- Asplund, S.O., 1949; "Strengthening of Bridge Slabs with Grouted reinforcement", *Journal of the American Concrete Institute*, V. 20, No. 6, pp. 397-406.
- Atkinson, R.H., and Schuller, M.P., 1992; "Development of Injectible Grouts for the Repair of Unreinforced Masonry", *Proceedings of the Workshop on Effectiveness of Retrofitting of Stone and Brick Masonry Walls in Seismic Areas*, Dept. of Struct. Engrg., Politecnico di Milano, Milan, Italy.
- De Lorenzis, L., Nanni, A., and La Tegola, A. (2000), "Flexural and Shear Strengthening of Reinforced Concrete Structures with Near Surface Mounted FRP Bars," Proc., Third Int. Conf. on Advanced Composite Materials in Bridges and Structures, Ottawa, Canada, pp. 521-528.
- De Lorenzis, L., and Nanni, A., 2001a; "Strengthening of Reinforced Concrete Beams with Near-Surface Mounted Fiber-Reinforced Polymer Bars", *Structural Journal*, ACI, V. 98, No. 1, pp. 60-68.
- De Lorenzis, L., and Nanni, A., 2001b; "Characterization of FRP Bars as Near Surface Mounted Reinforcement", *Journal of Composites for Construction*, ASCE, V. 5, No. 2, pp. 114-121.
- De Lorenzis, L., and Nanni, A., 2002; "Bond Between Near Surface Mounted FRP Bars and Concrete in Structural strengthening", *Structural Journal*, ACI, V. 99, No. 2, pp. 123-133.
- Emmons, P., Thomas, J., and Sabnis, G.M., 2001; "New Strengthening Technology for Blue Circle Cement Silo Repair and Upgrade", *Proceedings of FRP Workshop US-AID*, Cairo, Egypt.
- Gao, D., Benmokrane, B., and Tighiouart, B., 1998; "Bond Properties of FRP Rebars to Concrete", *Technical Report*, Department of Civil Engineering, University of Sherbrooke, Sherbrooke, Quebec, Canada, 27 pp.
- Garrity, S.W., 1995; "Retro-Reinforcement – A proposed repair System for Masonry Arch Bridges", *Proceedings of the First International Conference on Arch Bridges*, Bolton, UK, pp.557-566.
- Hassan, T., and Rizkalla, S.; "Investigation of Bond in Concrete Structures Strengthened with Near Surface Mounted CFRP Strips", *in press*.
- Hogue, T., Cornforth, R.C., and Nanni, A., 1999; "Myriad Convention Center Floor System Reinforcement", *Proceedings of the FRPRCS-4*, C.W. Dolan, S. Rizkalla and A. Nanni, Editors, ACI, Baltimore, MD, pp. 1145-1161.
- Khalifa, A., Gold, W.J., Nanni, A., and Abdel Aziz, M.I., 1998; "Contribution of Externally Bonded FRP to Shear Capacity of RC Flexural Member", *Journal of Composites for Construction*, ASCE, V. 2, No. 4, pp. 195-202.
- Ibell, T.J., and Valerio, P., 2002; "Shear Strengthening of Existing Concrete Bridges", *Proceedings of ICE Structures and Buildings*, UK, *in press*
- MacGregor, J.G., 1997a; "Reinforced Concrete: Mechanics and Design", *Third Edition*, Prentice-Hall, NJ, pp.388-392.
- MacGregor, J.G., 1997b; "Reinforced Concrete: Mechanics and Design", *Third Edition*, Prentice-Hall, NJ, pp.215-218.
- Nanni, A., Alkhrdaji, T., Barker, M., Chen, G., Mayo, R., and Yang, X., (1999). "Overview of Testing to Failure Program of a Highway Bridge Strengthened with FRP Composites", *Proceedings of Fourth International Symposium on Non-Metallic (FRP)*

Reinforcement for Concrete Structures (FRPRCS-4), SP-188, C. W. Dolan, S. Rizkalla, and A. Nanni, Eds., American Concrete Institute, Farmington Hills, Mich., pp. 69-75.

Prota, A, Nanni, A, Manfredi G, and Cosenza E, 2001. "Design Criteria for RC Beam-Column Joints Seismically Upgraded with Composites", *Proceedings of the International Conference on FRP Composites in Civil Engineering - CICE 2001*, J.-G. Teng, Ed., Hong Kong, China, V. 1, pp. 919-926.

Tumialan, G., Morbin, A., Nanni, A. and Modena, C., "Shear Strengthening of Masonry Walls with FRP Composites," COMPOSITES 2001 Convention and Trade Show, Composites Fabricators Association, October 3-6, 2001, Tampa, FL, CD-ROM, 6 pp.

Uppuluri, V.S., Bakis, C.E., Nanni, A., and Boothby, T.E., 1996; "Analysis of the Bond Mechanism in FRP Reinforcement Bars: The Effect of Bar Design and Properties", *Proceedings of the Second International Conference on Advanced Composite Materials in Bridges and Structures (ACMBS-II)*, Montreal, Canada, pp. 893-900.

Warren, G.E., 1998; "Waterfront Repair and Upgrade", Advanced Technology Demonstration Site No. 2: Pier 12, NAVSTA San Diego, Site Specific Report SSR-2419-SHR, Naval Facilities Engineering Service Center, Port Hueneme, CA.

APPENDIX I. EXAMPLE OF FLEXURAL DESIGN

Introduction

Flexural strengthening of a one-way RC slab supported by RC joists will be designed in this section. The eight-span floor slab was originally designed using a concrete compressive strength of 25.9 MPa (3750 psi) and steel reinforcement strength of 413.7 MPa (60 ksi). The slab thickness was selected equal to $h=180 \text{ mm}$ (7.25 in), using the dead and live loads reported in Table 2 (MacGregor, 1997a). The owner needs to modernize some mechanical equipment that becomes an integral part of the structure in the four central spans of the building (Figure 10). The new loads resulting from this equipment are shown in Table 2.

New moments due to the new loads are shown in Table 3. The moment in place (M_{ip}) at the time of FRP installation is calculated using the slab self weight and the weight due to the floor cover and ceiling. M_{new} represents the factored moment due to new loads to be resisted by the existing structure prior to the strengthening.

The original design called for 12-mm (#4) steel bars spaced 380 mm (15 in) on centers for positive moment regions, and 12-mm (#4) spaced at 300 mm (12 in) on centers for negative moment regions. Effective depth d and clear concrete cover were assumed equal to 160 mm (6.25 in) and 20 mm (0.75 in), respectively.

A 6-mm (#2) Carbon FRP bar is adopted for strengthening in the negative moment regions.

FRP guaranteed material properties and corresponding design values are shown in Eq. (2) based on the appropriate C_E factor (Table 1):

$$\begin{aligned}f_{fu} &= C_E f_{fu}^* = 0.95(1380 \text{ MPa}) = 1311 \text{ Mpa} \\ \varepsilon_{fu} &= C_E \varepsilon_{fu}^* = 0.95(0.01) = 9.5 \times 10^{-3} \\ E_f &= 138 \text{ GPa}\end{aligned}$$

Assuming 4 mm (0.125 in) clear cover, the effective depth is $d_f=173 \text{ mm}$ (6.8 in).

For positive moment regions, externally bonded FRP laminates will be used. This second technique is already well-known and outside the scope of this paper so that only the final results will be shown in this example.

Computations

As a first step, initial strain under the in-place moment needs to be evaluated. Neutral axis position before cracking (c_{b_cr}) and gross moment of inertia (I_g) of the concrete section are shown below (calculations are carried out for a strip of 300 mm (1 ft)):

$$\begin{aligned}
c_{b_cr} &= \frac{0.5bh^2 + (n-1)A_s d}{bh + (n-1)A_s} = \\
&= \frac{0.5(300\text{ mm})(180\text{ mm})^2 + (8.27-1)(129\text{ mm}^2)(160\text{ mm})}{300\text{ mm}(180\text{ mm}) + (8.27-1)(129\text{ mm}^2)} = 91\text{ mm} \\
I_g &= \frac{bh^3}{12} + (n-1)A_s(c_{b_cr} - d)^2 = \\
&= \frac{300\text{ mm}(180\text{ mm})^3}{12} + (8.27-1)(129\text{ mm}^2)(91\text{ mm} - 160\text{ mm})^2 = 150,265,008\text{ mm}^4
\end{aligned}$$

where:

$$n = \frac{E_s}{E_c} = \frac{E_s}{4750\sqrt{25.9\text{ MPa}}} = \frac{200,000\text{ MPa}}{24,174\text{ MPa}} = 8.27$$

Cracking moment is then obtained as:

$$M_{cr} = \frac{0.62\sqrt{f'_c} I_g}{h - c_{b_cr}} = \frac{1}{1 \times 10^6} \frac{0.62\sqrt{25.9\text{ MPa}} (150,265,009\text{ mm}^4)}{180\text{ mm} - 91\text{ mm}} = 5.33\text{ kN} \cdot \text{m}$$

Since service moment due to existing loads on the structure ($4.65\text{ kN} \cdot \text{m}$, Table 3) is smaller than M_{cr} analysis can be carried out referring to an uncracked cross-section. Consequently, initial strain in the bottom concrete fiber can be expressed as:

$$\varepsilon_{bi} = \frac{M_{ip}}{I_g E_c} (d_f - c_{b_cr}) = \frac{2,190,000\text{ N} \cdot \text{mm}}{(150,265,008\text{ mm}^4)(24,174\text{ MPa})} (173\text{ mm} - 91\text{ mm}) = 4.944 \times 10^{-5}$$

As a first trial, assume for the neutral axis position $c_l = 0.1h = 18\text{ mm}$, and that failure is controlled by FRP rupture, so that the maximum strain in the concrete surrounding FRP bars is given by the second term of Eq. (7):

$$\varepsilon_{c,f} = \varepsilon_{fe} + \varepsilon_{bi} = 6.650 \times 10^{-3} + 4.944 \times 10^{-5} = 6.699 \times 10^{-3}$$

where ε_{fe} is taken from Eq. (6):

$$\varepsilon_{fe} = \kappa_m \varepsilon_{fu} = 0.7(9.50 \times 10^{-3}) = 6.650 \times 10^{-3}$$

Strain level in both concrete and steel can be found using strain compatibility:

$$\varepsilon_c = \frac{c_1}{d_f - c_1} \varepsilon_{c,f} = \frac{18 \text{ mm}}{173 \text{ mm} - 18 \text{ mm}} (6.699 \times 10^{-3}) = 7.779 \times 10^{-4}$$

$$\varepsilon_s = \frac{d - c_1}{d_f - c_1} \varepsilon_{c,f} = \frac{160 \text{ mm} - 18 \text{ mm}}{173 \text{ mm} - 18 \text{ mm}} (6.699 \times 10^{-3}) = 6.137 \times 10^{-3}$$

Since $\varepsilon_s > \varepsilon_y = 2.07 \times 10^{-3}$, $f_s = f_y = 413.7 \text{ MPa}$, tensile forces in both steel and FRP reinforcement as well as compression force in the concrete can be expressed as follows:

$$T_f = A_f E_f \varepsilon_{fe} = (32.3 \text{ mm}^2) (1.38 \times 10^5 \text{ MPa}) (6.650 \times 10^{-3}) = 29,642 \text{ N}$$

$$T_s = A_s f_y = (129 \text{ mm}^2) (413.7 \text{ MPa}) = 53,367 \text{ N}$$

$$C_c = \alpha_1 f'_c \beta_1 c_1 b = 0.525 (25.9 \text{ MPa}) (0.85) (18 \text{ mm}) (300 \text{ mm}) = 62,410 \text{ N}$$

where:

$$\varepsilon'_c = 1.71 \frac{f'_c}{E_c} = 1.71 \frac{25.9 \text{ MPa}}{24,174 \text{ MPa}} = 1.832 \times 10^{-3}$$

$$\gamma_1 = \frac{4\varepsilon'_c - \varepsilon_c}{6\varepsilon'_c - 2\varepsilon_c} = \frac{4(1.832 \times 10^{-3}) - 7.779 \times 10^{-4}}{6(1.832 \times 10^{-3}) - 2(7.779 \times 10^{-4})} = 0.694$$

$$\alpha_1 = \frac{3\varepsilon'_c \varepsilon_c - \varepsilon_c^2}{3\varepsilon_c'^2 \gamma_1} = \frac{3(1.832 \times 10^{-3})(7.779 \times 10^{-4}) - (7.779 \times 10^{-4})^2}{3(1.832 \times 10^{-3})^2 (0.694)} = 0.525$$

Via equilibrium, one can find another position for the neutral axis:

$$T_s + T_f = C_c = \alpha_1 f'_c \beta_1 c_1' b$$

$$c_1' = \frac{T_s + T_f}{\alpha_1 f'_c \beta_1 b} = \frac{53,367 \text{ N} + 29,642 \text{ N}}{0.525 (25.9 \text{ MPa}) (0.85) (300 \text{ mm})} = 24 \text{ mm}$$

As a second trial, a new neutral axis depth is assumed:

$$c_2 = \frac{c_1 + c_1'}{2} = \frac{18 \text{ mm} + 24 \text{ mm}}{2} = 21 \text{ mm}$$

Repeating the calculations shown so far, using the value c_2 , one can find that equilibrium is satisfied and no further iterations are needed. Ultimate strain in concrete and steel is 9.254×10^{-4} and 6.127×10^{-3} , respectively; tensile force in FRP and steel reinforcement and compressive force in the concrete is 29,579 N, 53,365 N, and 82,944 N, respectively. To check whenever the original assumption of FRP rupture is correct the following shall be verified:

$$c < c_b = \frac{\varepsilon_{cu}}{\varepsilon_{cu} + \varepsilon_{c,f}} d_f = \frac{0.003}{0.003 + 6.699 \times 10^{-3}} (173 \text{ mm}) = 54 \text{ mm}$$

where c_b represents the neutral axis position for balanced failure. Being it verified, the initial assumption was correct.

The moment capacity can now be expressed as:

$$\begin{aligned} M_n &= A_s f_s \left(d - \frac{\beta_1 c}{2} \right) + \psi_f A_f f_{fe} \left(d_f - \frac{\beta_1 c}{2} \right) = \\ &= \frac{1}{1 \times 10^6} [129 \text{ mm}^2 (413.7 \text{ MPa}) (160 \text{ mm} - 0.85 (21 \text{ mm}) / 2) + \\ &+ 0.85 (32.3 \text{ mm}^2) (917.7 \text{ MPa}) (173 \text{ mm} - 0.85 (21 \text{ mm}) / 2)] = 12.2 \text{ kN} \cdot \text{m} \end{aligned}$$

where:

$$\begin{aligned} f_s &= E_s \varepsilon_s < f_y = 413.7 \text{ MPa} \\ f_{fe} &= E_f \varepsilon_{fe} = (1.38 \times 10^5 \text{ MPa}) (6.650 \times 10^{-3}) = 917.7 \text{ MPa} \end{aligned}$$

Because $\varepsilon_s > 0.005$, from Eq. (3) the strength reduction factor is $\phi = 0.9$. Finally,

$$\phi M_n = 0.9 (12.2 \text{ kN} \cdot \text{m}) = 11.0 \text{ kN} \cdot \text{m} > M_u = 10.2 \text{ kN} \cdot \text{m}$$

NSM bars used as reinforcement in negative moment regions will be extended for a length equal to their development length ℓ_d beyond the point of zero moment; ℓ_d can be evaluated using Eq. (18):

$$\ell_d = \frac{d_b}{4(0.5\tau_{\max})} f_{fe} = \frac{1}{1000} \frac{6 \text{ mm}}{4(0.5(3.5 \text{ MPa}))} 1237 \text{ MPa} \approx 1.0 \text{ m}$$

The point of zero is given at approximately $0.2 \cdot \ell$ where $\ell = 4.20 \text{ m}$ (13.83 ft). The total length of an FRP bar is given as: $2(0.2\ell) + 2\ell_d = 3.70 \text{ m}$ (12 ft).

For positive moment regions, design can be carried out using externally bonded CFRP laminates 100 mm (4 in) wide with strips clear spacing of 500 mm (20 in), having the following properties:

$$\begin{aligned} f_{fu} &= C_E f_{fu}^* = 0.95 (3800 \text{ MPa}) = 3610 \text{ MPa} \\ \varepsilon_{fu} &= C_E \varepsilon_{fu}^* = 0.95 (0.0167) = 0.0159 \\ E_f &= 228 \text{ GPa} \end{aligned}$$

The final strengthening design is reported in Table 3 and compared with the original design. Note that Eq. (1) is verified since ϕM_n of the existing member is larger than M_{new} calculated with the new loads in both positive and negative moment regions.

APPENDIX II. EXAMPLE OF SHEAR DESIGN

An existing simply supported T-beam supports a uniformly distributed service (unfactored) dead load of 19.0 N/mm (1.3 kips/ft), including its own weight and a uniformly distributed service live load of 23.4 N/mm (1.6 kips/ft), (MacGregor, 1997b). The concrete strength is 27.6 MPa (4000 psi), and the yield strength of the steel stirrups is 276 MPa (40 ksi). Overall height is $h=650 \text{ mm}$ (26 in), flange width is 910 mm (36 in), stem width is 300 mm (12 in), slab thickness is 150 mm (6 in), effective depth is $d=610 \text{ mm}$ (24 in), and clear concrete cover $c=40 \text{ mm}$ (1.5 in). The original shear design called for 10-mm ($\#3$) double-leg stirrups with the following spacing: *a*) one at 75 mm (3 in) from the support; *b*) seven at 150 mm (6 in); *c*) three at 200 mm (8 in); and *d*) nine at 300 mm (12 in) as shown in Figure 11.

The original flexural design called for two layers of longitudinal grade 60 steel bars used as main reinforcement; the bottom layer includes three 35-mm ($\#11$) steel bars; the top layer includes two 25-mm ($\#8$) steel bars. Two 12-mm ($\#4$) steel bars were used as compression reinforcement to hold the stirrups.

Service live load needs to be increased from 23.4 to 32.0 N/mm . Flexural capacity of the beam does not need to be improved, while an upgrading is needed in shear. The new ultimate shear value calculated at d from the support is 324.7 kN (73.0 kips).

Strengthening design will be carried out using 6.35-mm (*No. 2*) NSM CFRP bars 580 mm (23 in) long, having ultimate guaranteed tensile strength $f_{fu}^* = 2068 \text{ MPa}$ (300 ksi), modulus of elasticity $E_f = 124 \text{ GPa}$ ($18,000 \text{ ksi}$), and ultimate guaranteed elongation strain $\varepsilon_{fu}^* = 0.017$.

FRP contribution to the shear capacity of the beam is expressed by Eq. (11); FRP bars will be inserted between the existing steel stirrups leading to a center-to-center spacing of $s_f=80 \text{ mm}$ (3 in).

The number (n) of FRP bars crossed by a 45-degree shear crack is:

$$\begin{aligned} n &= \frac{\ell_{eff}(1 + \cot \alpha)}{s} = \frac{(\ell_b \sin \alpha - 2c)(1 + \cot \alpha)}{s} = \\ &= \frac{(500 \text{ mm} \cdot \sin(90) - 2(40 \text{ mm}))(1 + \cot(90))}{80 \text{ mm}} = 5.25 \Rightarrow n = 5 \end{aligned}$$

and the length where FRP bar strain governs ($l_{0.004}$) is:

$$l_{0.004} = 0.001 \frac{d_b E_f}{\tau_b} = 0.001 \frac{(6.35 \text{ mm})(124,000 \text{ MPa})}{6.9 \text{ MPa}} = 114 \text{ mm}$$

Finally from Eq. (12) and Figure 12 ($n/2 = 5/2 = 2.5 \Rightarrow n/2 = 2$):

$$\begin{aligned}
L_1 &= \min(l_{0.004}, s \cdot 1) = \min(114 \text{ mm}, (80 \text{ mm})(1)) = 80 \text{ mm} \\
L_2 &= \min(l_{0.004}, s \cdot 2) = \min(114 \text{ mm}, (80 \text{ mm})(2)) = 114 \text{ mm} \\
L_3 &= \min(l_{0.004}, \ell_{net} - s \cdot 3) = \\
&= \min[114 \text{ mm}, 420 \text{ mm} - (80 \text{ mm})(3)] = \min(114 \text{ mm}, 180 \text{ mm}) = 114 \text{ mm} \\
L_4 &= \min(l_{0.004}, \ell_{net} - s \cdot 4) = \\
&= \min[114 \text{ mm}, 420 \text{ mm} - (80 \text{ mm})(4)] = \min(114 \text{ mm}, 100 \text{ mm}) = 100 \text{ mm} \\
L_5 &= \min(l_{0.004}, \ell_{net} - s \cdot 5) = \\
&= \min[114 \text{ mm}, 420 \text{ mm} - (80 \text{ mm})(5)] = \min(114 \text{ mm}, 20 \text{ mm}) = 20 \text{ mm}
\end{aligned}$$

and

$$L_{tot} = L_1 + L_2 + L_3 + L_4 + L_5 = 80 + 114 + 114 + 100 + 20 = 428 \text{ mm}$$

FRP contribution to the shear capacity can now be expressed as (Eq. (11)):

$$V_f = 2\pi d_b \tau_b L_{tot} = (2)(3.14)(6.35 \text{ mm})(6.89 \text{ MPa})(428 \text{ mm}) = 117.6 \text{ kN}$$

To prevent concrete crushing, Eq. (17) shall be verified:

$$\begin{aligned}
V_s &= \frac{A_s f_y d}{s} = \frac{(142 \text{ mm}^2)(276 \text{ MPa})(610 \text{ mm})}{150 \text{ mm}} = 159.4 \text{ kN} \\
V_s + V_f &= 159.4 \text{ kN} + 117.6 \text{ kN} = 277 \text{ kN} < \\
&< 0.66\sqrt{f'_c} bd = 0.66\sqrt{27.6 \text{ MPa}}(300 \text{ mm})(610 \text{ mm}) = 634.5 \text{ kN}
\end{aligned}$$

Design shear capacity can be obtained using Eq. (10); a sketch showing the number and spacing of NSM CFRP bars selected for the shear strengthening is reported in Figure 13.

$$\begin{aligned}
\phi V_n &= \phi(V_c + V_s + \psi_f V_f) = \\
&= 0.85[160.2 \text{ kN} + 159.4 \text{ kN} + 0.85(117.6 \text{ kN})] = 356.6 \text{ kN} > V_u = 324.7 \text{ kN}
\end{aligned}$$

where:

$$V_c = \frac{\sqrt{f'_c}}{6} bd = \frac{\sqrt{27.6 \text{ MPa}}}{6} (300 \text{ mm})(610 \text{ mm}) = 160.2 \text{ kN}$$

NSM reinforcement is no longer needed 2.55 m (8.3 ft) apart from the support (Figure 13) since the existing steel stirrups are capable to carry the additional shear due to new loads.

APPENDIX III. NOTATION

a	=	Smallest dimension of a rectangular FRP bar;
A_f	=	Area of FRP reinforcement;
A_s	=	Area of steel reinforcement;
b	=	Larger dimension of a rectangular FRP bar, and cross-section width;
c	=	Neutral axis depth, Clear concrete cover;
c_b	=	Neutral axis depth for balanced failure;
c_{b_cr}	=	Neutral axis depth before cracking of the cross-section;
C_E	=	Environmental reduction factor;
d	=	Effective depth of steel reinforcement;
D	=	Dead Load;
d_b	=	Diameter of FRP bar;
d_f	=	Effective depth of FRP reinforcement;
d_{net}	=	Reduced value of the effective length of a FRP bar;
d_b	=	Length of a FRP NSM bar;
E_c	=	Modulus of elasticity of concrete;
E_f	=	Modulus of elasticity of FRP reinforcement;
E_s	=	Modulus of elasticity of steel reinforcement;
f_c'	=	Compressive strength of concrete;
f_{fe}	=	Effective tensile strength of FRP reinforcement;
f_{fu}	=	Ultimate design tensile strength of FRP reinforcement;
f_{fu}^*	=	Guaranteed tensile strength of FRP reinforcement;
f_s	=	Tensile strength of steel reinforcement;
f_y	=	Yielding strength of steel reinforcement;
h	=	Cross-section height;
I_g	=	Gross moment of inertia;
l	=	Length of the beam;
l_b	=	Length of FRP NSM bar;
l_d	=	Development length of FRP bars;
l_{eff}	=	Vertical length of FRP NSM bar used as shear reinforcement;
l_{net}	=	Net length of a FRP NSM bar used as shear reinforcement;
$l_{0.004}$	=	Length of FRP bar to maintain shear integrity of concrete;
L	=	Live load;
L_i	=	Length of each FRP bar crossed by a 45-degree shear crack;
L_{tot}	=	Total length of FRP bars crossed by a 45-degree shear crack;
M_n	=	Nominal moment strength at section;
M_{ip}	=	Moment in place at the time of FRP installation;
n	=	Modular ratio of elasticity E_s/E_c , and ratio defined by Eq. (15);
R_n	=	Nominal strength of the structure;
s	=	Spacing of steel and FRP shear reinforcement;
T_f	=	Tensile force in FRP reinforcement;
T_s	=	Tensile force in steel reinforcement;
V_c	=	Nominal shear strength provided by concrete;
V_f	=	Nominal shear strength provided by FRP reinforcement;

V_n	=	Nominal shear strength at section;
V_s	=	Nominal shear strength provided by steel reinforcement;
α	=	Angle between inclined FRP stirrups and longitudinal axis of member;
α_l	=	Coefficient of the Whitney stress block;
β_l	=	Coefficient of the Whitney stress block;
ε_{bi}	=	Initial strain in the concrete before FRP installation;
ε_c	=	Concrete compressive strain;
$\varepsilon_{c,f}$	=	Nominal tensile strain in concrete surrounding FRP bars;
ε_{cu}	=	Maximum permissible compressive strain in concrete (0.003);
ε_{fe}	=	Effective tensile strain in FRP reinforcement;
ε_{fu}	=	Ultimate design tensile strain of FRP reinforcement;
ε_{fu}^*	=	Guaranteed tensile strain of FRP reinforcement;
ε_s	=	Tensile strain of steel reinforcement;
ε_y	=	Yielding tensile strain of steel reinforcement;
κ_m	=	FRP Bond dependent coefficient for flexure;
ϕ	=	Strength-reduction factor;
ψ_f	=	Additional strength-reduction factor for FRP reinforcement;
τ_b	=	Average bond stress for FRP reinforcement;
τ_{max}	=	Maximum bond stress for FRP reinforcement.

List of Tables

Table 1 – Environmental-Reduction Factor C_E (ACI 440, 2002).....	22
Table 2 - Existing and New Loads.....	22
Table 3 - Original and Strengthening Design	22

List of Figures

Figure 1 - Strengthening of Cement Silos Using NSM Carbon FRP Bars	23
Figure 2 - Strengthening of a Bridge Deck Using NSM Carbon FRP	23
Figure 3 – Negative Moments Regions Strengthening of Bridge Deck with NSM Bars .	23
Figure 4 – Shear Strengthening of RC Joist Using Carbon NSM Bars	24
Figure 5 - Ultimate Internal Strain and Stress Distribution for Rectangular Sections.....	24
Figure 6 – NSM Installation	24
Figure 7 - FRP Bars Used as Shear Reinforcement.....	25
Figure 8 - Minimum Dimension of the Grooves	25
Figure 9 - Transfer of Force in an FRP Bar	25
Figure 10 - Typical Floor Plan and Cross-Section.....	25
Figure 11 – Steel Stirrups in Beam	26
Figure 12 - Definition of L_i for a 80 mm Bar Spacing (Only NSM Bars are shown)	26
Figure 13 - Shear Upgrading Using NSM CFRP Bars (Only NSM Bars are shown)	26

Table 1 – Environmental-Reduction Factor C_E (ACI 440, 2002)

Exposure condition	Fiber and resin type	C_E
Interior exposure	Carbon/epoxy	0.95
	Glass/epoxy	0.75
	Aramid/epoxy	0.85
Exterior exposure (bridges, piers, and unenclosed parking garages)	Carbon/epoxy	0.85
	Glass/epoxy	0.65
	Aramid/epoxy	0.75
Aggressive environment (chemical plants and waste water treatment plants)	Carbon/epoxy	0.85
	Glass/epoxy	0.50
	Aramid/epoxy	0.70

Table 2 - Existing and New Loads

	US Units		SI Units	
	Existing Loads [psf]	New Loads [psf]	Existing Loads [kN/m ²]	New Loads [kN/m ²]
Slab self weight	90.6	90.6	4.34	4.34
Floor cover	0.5	0.5	0.024	0.024
Mechanical equipment	4.0	95.0	0.192	4.55
Ceiling	2.0	2.0	0.096	0.096
Dead load, ω_d	97.1	188.1	4.65	9.00
Live load, ω_l	100.0	100.0	4.80	4.80
Factored load, ω_u	306	433	14.66	20.74
Service load, ω_s	197	288	9.44	13.80
In place load, ω_{ip}	---	93	---	4.46
New load from Eq. (1), ω_{new}	---	310	---	14.85

Table 3 - Original and Strengthening Design

	US Units		SI Units	
	M^+ [k-ft]	M^- [k-ft]	M^+ [kN·m]	M^- [kN·m]
Existing Load				
Service Moment, M_s	2.36	3.43	3.20	4.65
Ultimate Moment, M_u	3.66	5.32	4.96	7.21
Flexural Capacity, ϕM_n	4.40	5.50	5.96	7.45
New Loads				
Service Moment, M_s	3.44	5.01	4.66	6.79
Moment in Place, M_{ip}	1.11	1.62	1.50	2.19
Moment from Eq. (1), M_{new}	3.71	5.40	5.03	7.32
Ultimate Moment, M_u	5.18	7.53	7.02	10.20
Flexural Capacity, ϕM_n	7.07	8.12	9.58	12.20



Figure 1 - Strengthening of Cement Silos Using NSM Carbon FRP Bars



Figure 2 - Strengthening of a Bridge Deck Using NSM Carbon FRP



Figure 3 – Negative Moments Regions Strengthening of Bridge Deck with NSM Bars



Figure 4 – Shear Strengthening of RC Joist Using Carbon NSM Bars

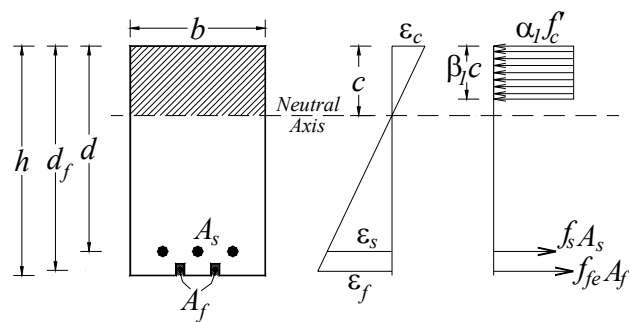


Figure 5 - Ultimate Internal Strain and Stress Distribution for Rectangular Sections

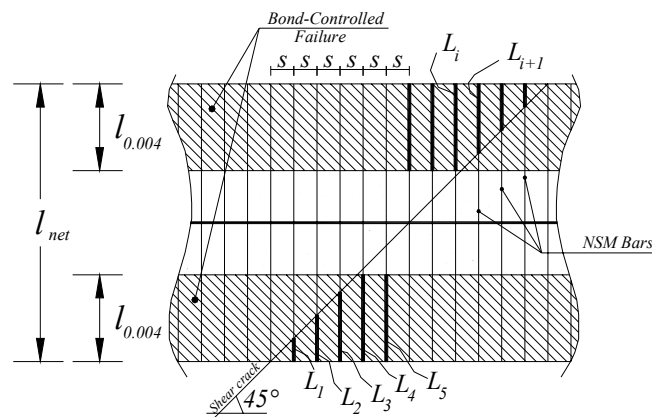


Figure 6 – NSM Installation

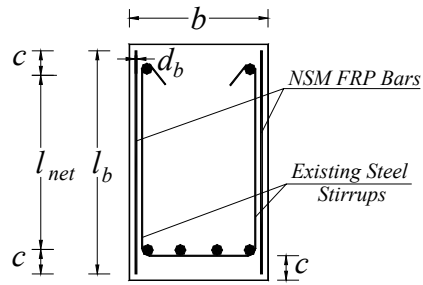


Figure 7 - FRP Bars Used as Shear Reinforcement

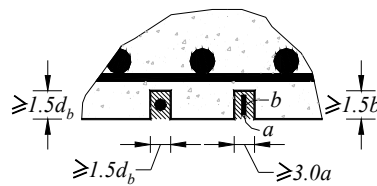


Figure 8 - Minimum Dimension of the Grooves

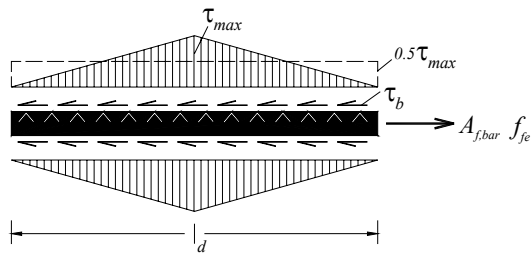


Figure 9 - Transfer of Force in an FRP Bar

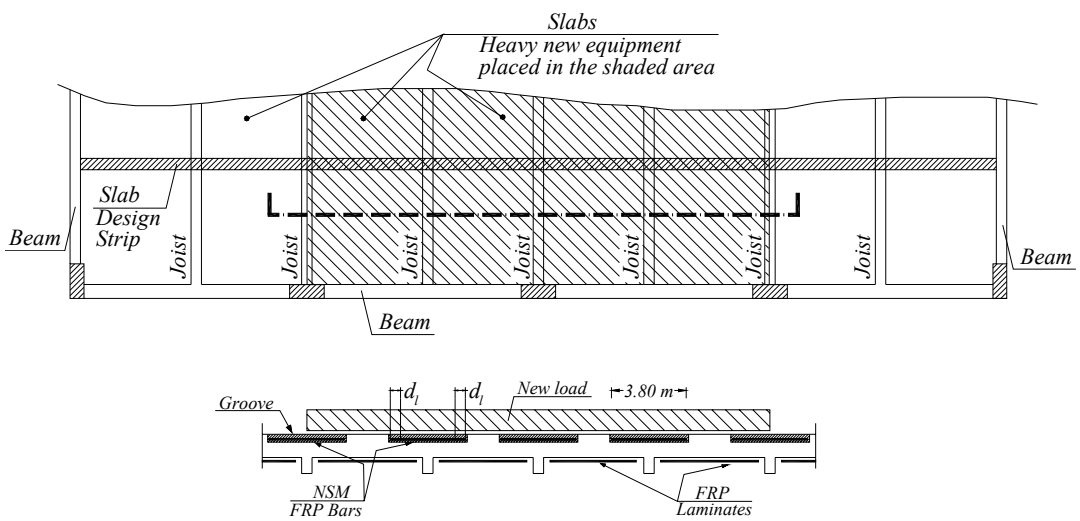


Figure 10 - Typical Floor Plan and Cross-Section

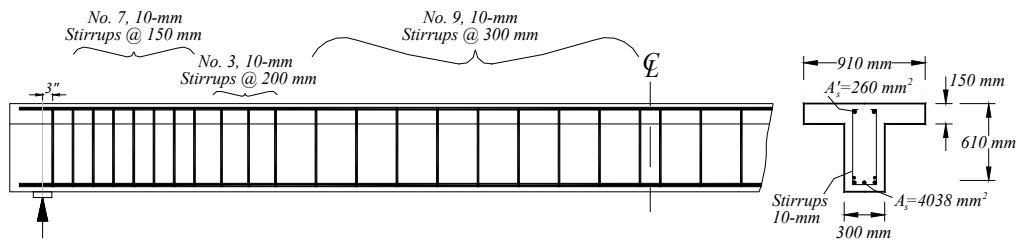


Figure 11 – Steel Stirrups in Beam

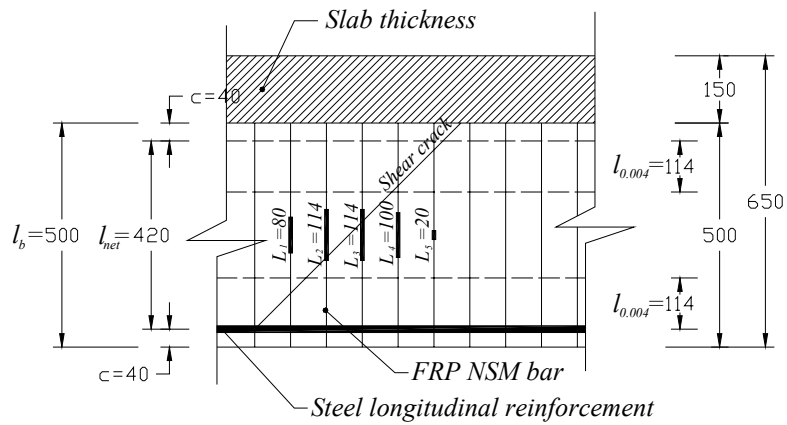


Figure 12 - Definition of L_i for a 80 mm Bar Spacing (Only NSM Bars are shown)

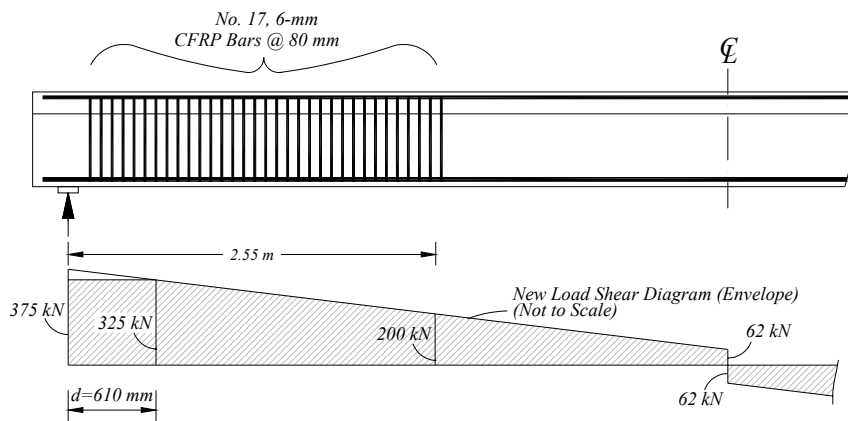


Figure 13 - Shear Upgrading Using NSM CFRP Bars (Only NSM Bars are shown)